

TIDE: Task-Isolated Diffusion for Unified Video Editing and Generation

Qi Liu^{1,*} Gang Yue^{2,*} Mingyu Yin² Lisai Zhang² Yidi Wu²
Yaole Wang² Yaohui Wang² Chang Yao¹ Jingyuan Chen^{1,†} Lin Ma[†]

¹Zhejiang University ²Bilibili Inc.

*Equal contribution †Corresponding author

{qiliu, changyao, jingyuanchen}@zju.edu.cn



Figure 1: TIDE unifies instruction-based editing, reference-guided editing, and multi-reference generation.

Abstract

Recent advances in Diffusion Transformers have driven rapid progress in video generation and editing, yet these capabilities are still handled by separate, task-specific models. Building a unified framework that supports diverse video tasks remains an open challenge: existing unified attempts either require dedicated auxiliary encoders or lack explicit mechanisms to distinguish heterogeneous conditioning tokens, struggling when the number and type of visual conditions vary across tasks. We propose TIDE, a unified framework that integrates instruction-based editing, reference-guided editing, and multi-reference generation. At its core, we introduce

per-token task embeddings that assign each input token a task-specific identifier, enabling the model to explicitly disambiguate target, source, and reference tokens. To simultaneously capture high-level semantic understanding and fine-grained structural fidelity, we design a dual-path conditioning scheme that couples a vision-language model with a VAE latent path for complementary signals. We further devise a multi-task progressive training strategy that incrementally introduces tasks of increasing complexity, effectively harmonizing diverse objectives and enabling smooth generalization across heterogeneous task distributions. Extensive experiments on multiple video editing and generation benchmarks demonstrate that TIDE achieves state-of-the-art performance across all evaluated tasks. Our project page is available at <https://LittleWork123.github.io/tide>.

1 Introduction

The rapid evolution of Diffusion Transformers (DiTs) Peebles and Xie (2022) has propelled video synthesis to a new level, with large-scale models Wan et al. (2025); Kong et al. (2024); Yang et al. (2024); HaCohen et al. (2026) achieving impressive text-to-video and image-to-video generation. Beyond foundational generation, a proliferation of downstream capabilities has emerged, notably *instruction-based video editing* Cheng et al. (2023); He et al. (2025a); Bai et al. (2025a); Team (2025); Liao et al. (2025); Wu et al. (2025b); Tan et al. (2025) and *subject-reference video generation* Liu et al. (2025); Guo et al. (2026). However, these capabilities are still handled by separate, task-specific models Chen et al. (2026b), and building a unified framework that supports diverse video tasks remains an open challenge. In the image domain, researchers have begun constructing unified architectures Xiao et al. (2024); Chen et al. (2024) that integrate generation, editing, and reference-guided tasks into a cohesive system. In the video domain, recent works including VACE Jiang et al. (2025), VINO Chen et al. (2026b), and DreamID-Omni Guo et al. (2026) represent initial steps toward unified video models, yet they either require dedicated auxiliary encoders or lack explicit mechanisms to prevent inter-task interference.

A closer look reveals that these seemingly disparate tasks can be cast as a *single conditional denoising problem with varying token roles*: the model receives a mixed sequence of target, source, and reference tokens and must learn which to reconstruct, which to preserve, and which to draw identity from. The key challenge lies in enabling the model to correctly distinguish these roles. Existing approaches adopt different strategies: VACE Jiang et al. (2025) introduces a dedicated context encoder to process conditioning signals separately; VINO Chen et al. (2026b) uses a structured 3D RoPE layout with special boundary tokens to distinguish heterogeneous visual sources in the attention sequence. However, these designs either require carefully engineered positional encoding schemes or additional encoder modules, and can struggle when the number of conditioning sources varies (e.g., multi-reference editing with multiple reference images).

Realizing this unified vision, however, requires overcoming three concrete obstacles: (1) **Conditioning disambiguation**: when multiple visual inputs (source video, reference images) are concatenated into a shared attention sequence, the model lacks cues to determine which tokens should be preserved, which provide identity, and which are denoising targets. VACE Jiang et al. (2025) observes that explicitly separating data of different modalities and distributions is essential for model convergence, while VINO Chen et al. (2026b) reports that without boundary marking, concatenated latents lead to identity swapping and attribute leakage. (2) **Conditioning duality**: reference-guided tasks simultaneously demand high-level semantic understanding (interpreting *what* to generate from text and reference) and fine-grained structural fidelity (preserving *how* it should look), yet no single conditioning pathway can satisfy both Hu et al. (2025); Zhong et al. (2025). (3) **Data scarcity and task conflicts**: existing editing datasets He et al. (2025a); Bai et al. (2025a) provide source-target pairs with instructions but lack reference images, and multi-task training risks inter-task degradation from conflicting learning objectives Guo et al. (2026) without careful curriculum design.

To address these challenges, we introduce **TIDE**, a unified framework that integrates instruction-based editing, reference-guided editing, and multi-reference generation. Central to TIDE is a *per-token task embedding*: a learnable embedding table that assigns each input token a task-specific identifier, enabling the model to explicitly distinguish target, source, and reference tokens. Crucially, the same type of visual input (e.g., a reference image) receives different identifiers depending on the task

context, and each reference in multi-reference scenarios is assigned a unique identifier, allowing the model to differentiate multiple visual identities.

Complementing the task isolation, we design a *dual-path conditioning* scheme that combines a semantic path (encoding references jointly with text instructions through Gemma-3-12B-IT Team et al. (2025a) for high-level intent understanding) with a latent path (encoding references through the Video VAE for fine-grained structural and textural detail). The two paths address the conditioning duality: semantic guidance alone cannot preserve detailed visual appearance Hu et al. (2025), while latent conditioning alone lacks the capacity to interpret complex instructions Zhong et al. (2025); HaCohen et al. (2026).

Finally, to harmonize tasks with varying conditioning strengths, we adopt a *multi-task progressive training* strategy that incrementally introduces tasks of increasing complexity, preventing the model from overfitting to any single task while maintaining strong performance across all tasks.

In summary, our contributions are as follows:

1. We propose TIDE, a unified video editing and generation framework that seamlessly integrates instruction-based editing, reference-guided editing, and multi-reference generation through a shared conditional denoising formulation.
2. We introduce per-token task embeddings that assign each input token a task-specific identifier, enabling the model to explicitly disambiguate heterogeneous conditioning tokens.
3. We design a dual-path conditioning scheme that couples VLM-based semantic guidance with VAE-based latent-space detail injection, complemented by a multi-task progressive training strategy that effectively harmonizes tasks with varying conditioning requirements.
4. Extensive experiments demonstrate that TIDE achieves state-of-the-art performance on OpenVE-Bench and OpenS2V. We also contribute TIDE-Bench, a new benchmark for evaluating multi-reference video editing, on which TIDE substantially outperforms existing methods.

2 Related Work

Video Diffusion Models. Early video diffusion models Ho et al. (2022); Singer et al. (2022) extend image diffusion to the temporal axis via 3D U-Net architectures, demonstrating the viability of denoising-based video synthesis. Subsequent latent-space approaches Blattmann et al. (2023); Guo et al. (2023) reduce computational cost by operating in a compressed latent space, enabling higher resolution and longer generation. More recently, the Diffusion Transformer (DiT) Peebles and Xie (2022) paradigm has emerged as the dominant backbone: Latte Ma et al. (2024) first applies DiT to latent video generation, while Sora Brooks et al. (2024) demonstrates that scaling DiT with 3D spatiotemporal patches yields remarkable visual quality and temporal coherence. This architecture has been widely adopted by open-source and industrial models alike Yang et al. (2024); Zheng et al. (2024); Kong et al. (2024); Wan et al. (2025); Polyak et al. (2024); HaCohen et al. (2026), which pair 3D VAEs for spatiotemporal compression with DiT-based denoising and flow matching Lipman et al. (2022) objectives. Our work builds on LTX-2 HaCohen et al. (2026) and extends it into a unified multi-task framework for both editing and generation.

Video Editing. Training-free methods Song et al. (2020); Qi et al. (2023); Geyer et al. (2023); Kara et al. (2024) leverage pretrained priors via inversion and attention manipulation but are limited to global edits. Training-based approaches Team (2025); Liao et al. (2025); Yu et al. (2025); Wang et al. (2026b) learn from large-scale paired datasets He et al. (2025a); Bai et al. (2025a); Wu et al. (2025b); Zi et al. (2025) with complementary benchmarks Li et al. (2025a). Recent works unify multiple tasks within a single model: VACE Jiang et al. (2025) adds a unified context encoder to Wan-14B; VINO Chen et al. (2026b) couples a VLM with an MMDiT via learnable query tokens and token boundaries; Omni-Video 2 Yang et al. (2026) and Tele-Omni Liu et al. (2026) scale MLLM-conditioned diffusion for compositional editing; Many-for-Many Yang et al. (2025) and FullDiT2 He et al. (2025b) explore efficient in-context conditioning. However, these methods either require heavyweight auxiliary encoders or rely on implicit conditioning without explicit task-level isolation. Our per-token task embedding provides lightweight, explicit task-level isolation.

Reference-Based Video Generation and Editing. Early adapter-based approaches Ye et al. (2023) decouple image prompting from text-conditioned diffusion via cross-attention. In subject-to-video (S2V) generation, methods have progressed from single-identity Liu et al. (2025) to multi-subject

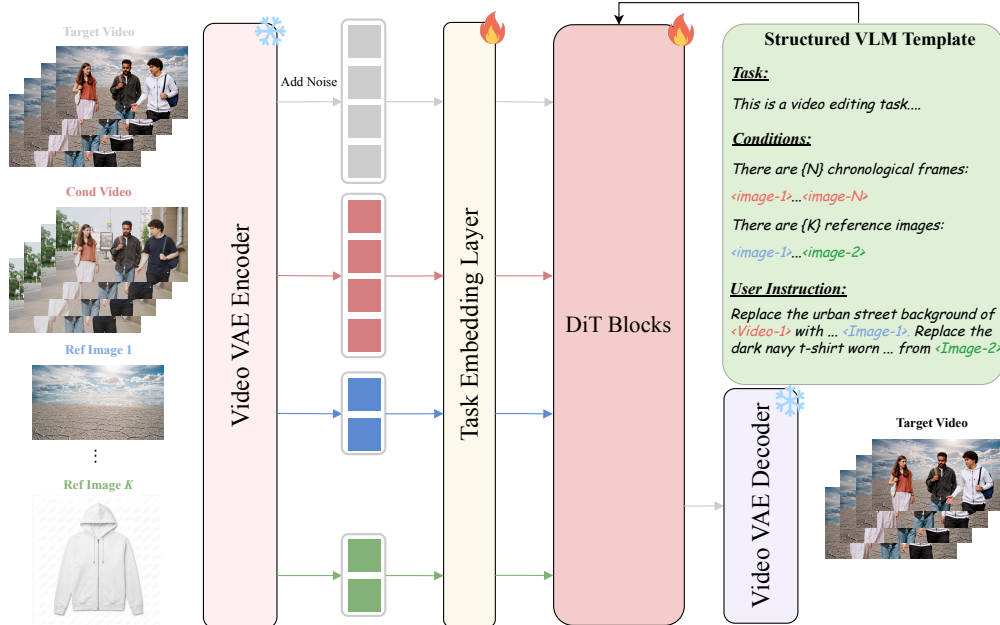


Figure 2: **Overview of TIDE.** Per-token task embeddings isolate heterogeneous conditioning tokens within shared self-attention (**Left**), while dual-path conditioning combines VLM-based semantic guidance with VAE-encoded latent detail (**Right**).

settings Huang et al. (2025); Li et al. (2025b); Zhu et al. (2026); Chen et al. (2025b); Girish et al. (2025); Fei et al. (2025); Song et al. (2026); Cai et al. (2025); Deng et al. (2025); Yuan et al. (2025); Hu et al. (2025), with increasing support for flexible composition and fine-grained control. For reference-guided editing, MiVE Wang et al. (2026a) repurposes VLMs as multiscale feature extractors, DreamID-Omni Guo et al. (2026) unifies human-centric generation and editing via symmetric conditioning, and other works Zhong et al. (2025) concatenate reference latents directly with target latents. In the image domain, OmniGen Xiao et al. (2024) and UniReal Chen et al. (2024) demonstrate that generation, editing, and reference tasks can co-exist in a single model, motivating similar unification in the video domain. Our approach supports arbitrary numbers of references through per-reference task embeddings and unifies generation and editing within a cohesive DiT-VLM framework.

3 Method

We formalize the problem as a single conditional denoising formulation (§3.1), then describe per-token task embeddings (§3.2), dual-path conditioning (§3.3), and the training procedure (§3.4).

3.1 Problem Formulation

We cast reference-based video generation and video editing as a single conditional denoising problem. Given a text prompt \mathcal{T} , optional conditioning visual latents $\mathcal{V} = \{V_1, \dots, V_K\}$ encoded via a 3D VAE, and per-token task identifiers τ , our model learns:

$$P(Y | \mathcal{T}, \mathcal{V}, \tau), \quad (1)$$

where Y denotes the target video. By selectively providing conditioning signals and assigning appropriate task identifiers, this formulation covers subject-reference video generation, reference-guided video editing, and instruction-based video editing (Table 1).

As illustrated in Figure 2, TIDE builds upon LTX-2 HaCohen et al. (2026) with a 3D Video VAE, a 48-block DiT backbone, and Gemma-3-12B-IT Team et al. (2025a) as the vision-language encoder. TIDE introduces two mechanisms on top of this backbone: per-token task embeddings (§3.2) and dual-path conditioning (§3.3).

Table 1: Task unification in TIDE. The same visual input receives *different* task identifiers τ depending on the task.

Task	Conditions	Task IDs (τ)	Output
Subject-Ref. Video Gen.	$\mathcal{T}, \{V_k^{\text{ref}}\}$	ref: $\tau_1^g, \tau_2^g, \dots$	Video
Ref-Guided Video Editing	$\mathcal{T}, V_{\text{src}}, \{V_k^{\text{ref}}\}$	src: τ_s^e , ref: τ_1^e, \dots	Video
Instruction-Based Video Editing	$\mathcal{T}, V_{\text{src}}$	src: τ_s^e	Video

3.2 Per-Token Task Embedding

Unifying multiple tasks introduces a fundamental tension: subject-reference generation requires the model to faithfully preserve reference identity, while editing demands selective modification of source content. Without an explicit signal to distinguish these conditioning roles, the model conflates preservation with modification, leading to inter-task interference. Existing methods address this via dedicated auxiliary encoders Jiang et al. (2025) or carefully designed positional encoding with boundary tokens Chen et al. (2026b), but these approaches can be difficult to extend when the number of conditioning sources varies across tasks.

We introduce a learnable task embedding table $\mathbf{E} \in \mathbb{R}^{N \times D}$, where N is the number of task slots and D the hidden dimension. For each patchified latent token \mathbf{h}_i with assigned task identifier τ_i , the task-conditioned representation is:

$$\tilde{\mathbf{h}}_i = \mathbf{h}_i + \mathbf{E}[\tau_i] \cdot \mathbb{1}[\tau_i \neq 0], \quad (2)$$

where $\mathbf{E}[\tau_i]$ indexes the τ_i -th row. This design ensures that target tokens ($\tau=0$) receive zero perturbation, exactly preserving the pretrained model’s generation behavior, while each conditioning token receives a learned embedding that signals its role to the attention mechanism.

Identifiers are assigned at the *token level* and partitioned into contiguous ranges for different conditioning roles. For subject-reference generation, each reference image receives a unique identifier ($\tau_1^g, \tau_2^g, \dots$); for editing tasks, the source video and reference images receive identifiers from a separate range (τ_s^e for source, $\tau_1^e, \tau_2^e, \dots$ for references). Crucially, the same type of visual input receives *different* identifiers depending on the task context: a reference image used in subject-to-video generation and the same image used in reference-guided editing are assigned different identifiers, enabling the model to learn task-appropriate behavior for each conditioning role. For multi-reference tasks, each reference occupies a unique identifier, allowing the model to differentiate multiple visual identities. Extending to new tasks requires only allocating new identifiers and providing corresponding training data.

3.3 Dual-Path Conditioning

Reference-guided tasks simultaneously demand high-level semantic understanding (interpreting *what* to generate from text and reference) and fine-grained structural fidelity (preserving *how* it should look). No single conditioning pathway satisfies both Hu et al. (2025); Zhong et al. (2025): VLM-based encoding excels at capturing semantic intent but compresses fine visual details, while VAE-based latent encoding retains structural information but cannot interpret complex instructions. We therefore design a dual-path scheme that injects complementary signals through two channels.

Semantic Path. The VLM path jointly encodes visual conditions with the text instruction through Gemma-3-12B-IT, producing contextualized embeddings that capture the semantic relationship between visual inputs and the generation or editing intent. We design task-specific structured prompt templates (illustrated in Figure 2). For subject-reference generation, reference images are interleaved with descriptive anchors within the VLM input. For editing tasks, N frames uniformly sampled from the source video ($N=5$ by default) replace the reference slots to provide temporal context, and for reference-guided editing, subject reference images are additionally appended after the source frames. The VLM outputs are projected through the Embeddings Connector and serve as keys and values for cross-attention in each DiT block, providing high-level semantic guidance that is difficult to derive from latent-space conditioning alone.

Latent Path. The latent path encodes all visual inputs through the 3D Video VAE and concatenates them into a single token sequence within the self-attention. For reference-guided editing, the complete

sequence takes the form:

$$\mathbf{X} = [\underbrace{\mathbf{H}_{\text{target}}}_{\tau=0}; \underbrace{\mathbf{H}_{\text{src}}}_{\tau_s^e}; \underbrace{\mathbf{H}_{\text{ref}_1}}_{\tau_1^e}; \underbrace{\mathbf{H}_{\text{ref}_2}}_{\tau_2^e}; \dots], \quad (3)$$

where $[\cdot]$ denotes sequence concatenation. For subject-reference generation, the source term is absent and reference tokens receive generation-specific identifiers (τ_k^g instead of τ_k^e). Each conditioning source receives its dedicated task identifier from Eq. (2), enabling the model to distinguish tokens from different sources. This is the key distinction from prior work HaCohen et al. (2026); Guo et al. (2026); Jiang et al. (2025) that concatenates all conditioning tokens without task-level differentiation. A binary conditioning mask $\mathbf{m} \in \{0, 1\}^L$ keeps conditioning tokens noise-free ($\sigma_i=0$) while target tokens receive diffusion noise ($\sigma_i=\sigma$), and the training loss is computed exclusively over target tokens.

Together, the two paths form a complementary conditioning system: the semantic path provides high-level understanding of editing intent via cross-attention, guiding *what* to generate, while the latent path preserves fine-grained structural detail via self-attention with task isolation, ensuring *how* it should look while preventing interference between conditioning sources. Ablation studies in §4.4 confirm that removing either path leads to significant degradation.

3.4 Training and Inference

Multi-Task Progressive Training. Naively mixing all tasks from the start risks inter-task degradation, as editing objectives can conflict with generation objectives during early optimization Guo et al. (2026). We adopt a three-stage progressive strategy that incrementally introduces tasks of increasing complexity. Stage 1 trains exclusively on instruction-based editing to establish basic editing capability. Stage 2 introduces the full multi-task mixture, including reference-guided editing, subject-to-video generation, and multi-reference tasks, to warm up multi-task representations. Stage 3 continues multi-task training with refined sampling ratios and a reduced learning rate for long-horizon convergence. This progressive curriculum allows the model to first consolidate basic editing competence before adapting to the more challenging multi-reference scenarios. Detailed step counts, learning rates, and data ratios are reported in §4.1 and Appendix D.

Objective. We adopt flow matching Lipman et al. (2022) with shifted logit-normal timestep sampling. Given a clean sample \mathbf{x}_0 and noise $\epsilon \sim \mathcal{N}(0, \mathbf{I})$, the noisy sample at timestep σ is $\mathbf{x}_\sigma = (1-\sigma)\mathbf{x}_0 + \sigma\epsilon$. The model predicts the velocity field $\mathbf{v} = \epsilon - \mathbf{x}_0$, and the training loss is:

$$\mathcal{L} = \mathbb{E}_{\sigma, \epsilon} \left[\frac{1}{|\mathcal{S}|} \sum_{i \in \mathcal{S}} \|\mathbf{v}_\theta(\mathbf{x}_\sigma, \mathbf{c}, \boldsymbol{\tau}, \sigma)_i - (\epsilon - \mathbf{x}_0)_i\|^2 \right], \quad (4)$$

where $\mathcal{S} = \{i : \mathbf{m}_i = 0\}$ denotes target token indices, ensuring that the model is trained only to reconstruct the target video while leaving conditioning tokens unchanged.

Inference. At inference time, we employ classifier-free guidance (CFG) combined with spatiotemporal guidance (STG) Hong (2024):

$$\hat{\mathbf{v}} = \mathbf{v}_{\text{uncond}} + s_{\text{cfg}}(\mathbf{v}_{\text{cond}} - \mathbf{v}_{\text{uncond}}) + s_{\text{stg}}(\mathbf{v}_{\text{cond}} - \mathbf{v}_{\text{stg}}), \quad (5)$$

where $s_{\text{cfg}}=4.0$ and $s_{\text{stg}}=1.0$. We use a 50-step Euler schedule, generating videos at 1280×704 resolution.

4 Experiments

4.1 Experimental Setup

Implementation Details. We build TIDE on top of LTX-2.3 HaCohen et al. (2026), using its native Gemma-3-12B-IT Team et al. (2025a) as the VLM encoder (frozen throughout training) and its 14B-parameter DiT backbone, which is fully fine-tuned together with randomly initialized task embedding tables. Training proceeds through three progressive stages (Stage 1: $\sim 3\text{K}$ steps, Stage 2: $\sim 7\text{K}$ steps, Stage 3: $\sim 10\text{K}$ steps) on H20 GPUs with FSDP; detailed hyperparameters, data ratios, and per-category data counts are provided in Appendix D. At inference, we use CFG with $s_{\text{cfg}}=4.0$. For generation tasks, we produce 145-frame videos at 24 fps and 1280×704 resolution; for editing tasks, the frame count and resolution follow the source video from each benchmark.

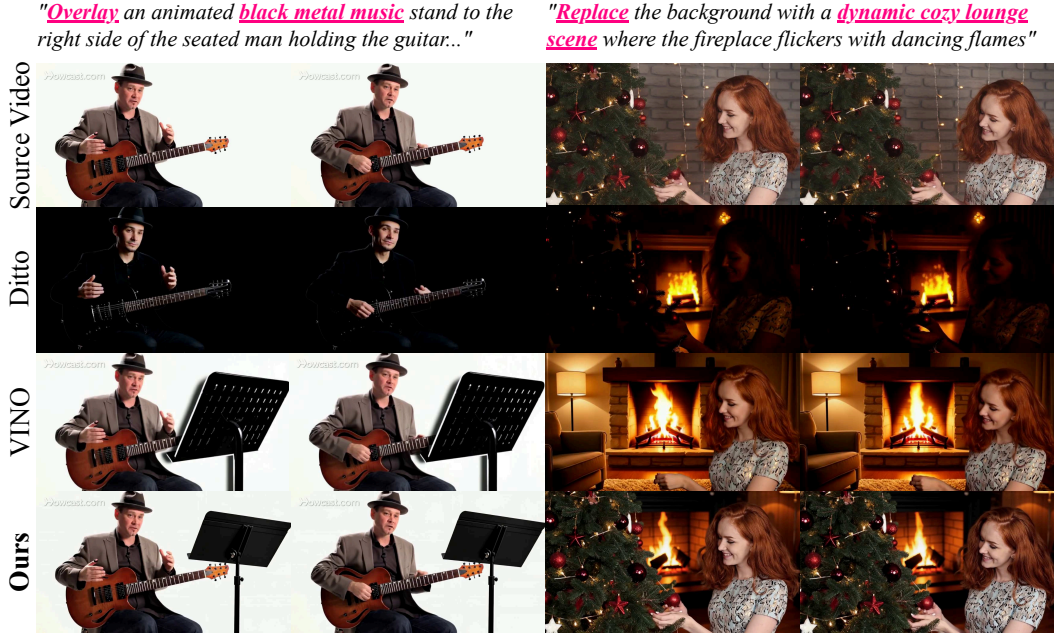


Figure 3: **Qualitative comparison** on OpenVE-Bench.

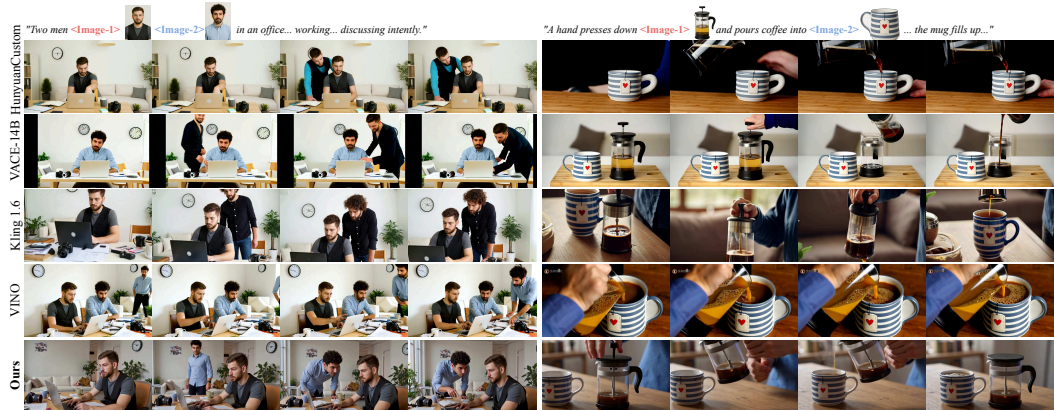


Figure 4: **Qualitative comparison** on multi-reference subject-to-video generation.

Benchmarks and Metrics. We evaluate on three benchmarks. **OpenVE-Bench** He et al. (2025a) covers 8 instruction-based video editing categories, scored by Gemini-3.1-Pro Comanici et al. (2025) as an LLM judge. **OpenS2V** Liu et al. (2025) evaluates subject-to-video generation via Aesthetics (visual appeal), Motion Smoothness/Amplitude (temporal quality), GME (motion coherence), Nexus (subject-text alignment), and Naturalness (physical plausibility), aggregated into a weighted Total score. **TIDE-Bench** (ours) targets multi-reference video editing across diverse editing combinations, evaluated by Gemini-3.1-Pro on Edit Completeness, Reference Faithfulness, Visual & Temporal Quality, Scene Preservation, and Overall Quality (details in Appendix C).

Baselines. For instruction-based editing (OpenVE-Bench), we compare with open-source methods InsVIE Wu et al. (2025b), DITTO Bai et al. (2025a), Lucy-Edit Team (2025), ICVE Liao et al. (2025), Omni-Video Tan et al. (2025), VINO Chen et al. (2026b), and closed-source Kling-O1 Team et al. (2025b) and SkyReels-Omni Chen et al. (2026a). For multi-reference editing (TIDE-Bench), we compare with VINO as the only open-source method that natively supports this setting, along with closed-source Kling-O1 Team et al. (2025b) and SkyReels-Omni Chen et al. (2026a). For subject-to-video generation (OpenS2V), we compare with MagRef Deng et al. (2025), Phantom Liu

Table 2: Comparison with SOTA methods on OpenVE-Bench.

Method	Style	BG	Chg	Rm	Add	Sub	Cre	Cam	Avg.
<i>Closed-source</i>									
Kling-O1 Team et al. (2025b)	4.32	2.44	4.01	3.03	2.89	3.12	3.44	3.75	3.36
SkyReels-Omni Chen et al. (2026a)	4.41	2.23	4.19	3.35	2.36	3.62	3.44	1.23	3.14
<i>Open-source</i>									
InsVIE Wu et al. (2025b)	1.40	1.00	1.29	1.00	1.04	1.17	1.50	1.04	1.16
DITTO Bai et al. (2025a)	3.72	1.09	1.87	1.00	1.39	1.09	2.35	1.05	1.68
Lucy-Edit Team (2025)	2.33	1.33	2.80	1.14	2.01	1.06	2.46	1.00	1.78
ICVE Liao et al. (2025)	2.40	1.18	2.23	1.85	1.75	2.24	2.09	1.01	1.84
Omni-Video Tan et al. (2025)	3.07	1.11	2.37	1.39	1.87	2.33	<u>2.92</u>	1.77	2.05
VINO Chen et al. (2026b)	4.31	1.50	2.94	<u>2.38</u>	<u>2.07</u>	<u>2.78</u>	2.63	2.22	<u>2.60</u>
TIDE (Ours)	4.32	2.62	3.54	2.68	2.18	3.56	2.93	<u>1.15</u>	2.91

Table 3: Comparison with SOTA methods on TIDE-Bench.

Method	Edit \uparrow	Ref \uparrow	V&T \uparrow	Pres \uparrow	Qual \uparrow	Avg. \uparrow
<i>Closed-source</i>						
Kling-O1 Team et al. (2025b)	4.09	3.78	3.43	3.47	3.40	3.63
SkyReels-Omni Chen et al. (2026a)	4.29	4.01	3.58	3.63	3.53	3.81
<i>Open-source</i>						
VINO Chen et al. (2026b)	<u>3.05</u>	<u>2.73</u>	<u>2.27</u>	<u>2.14</u>	<u>2.07</u>	<u>2.45</u>
TIDE (Ours)	4.07	3.44	3.20	3.21	3.15	3.41

et al. (2025), SkyReels Chen et al. (2025a), VACE Jiang et al. (2025), HunyuanCustom Hu et al. (2025), VINO Chen et al. (2026b), and closed-source Kling 1.6 Team et al. (2025b), Pika 2.1 Pika Labs (2025), and Vidu 2.0 Shengshu Technology (2025).

4.2 Quantitative Results

Instruction-Based Video Editing. As demonstrated in Table 2, TIDE achieves the best average score among all open-source methods, outperforming the previous best VINO by a clear margin. Notably, TIDE leads all methods in background change and subtitle editing, and matches Kling-O1 on global style transfer. The improvement is particularly pronounced on fine-grained local edits (Chg, Add, Rm), indicating that the dual-path conditioning effectively captures both semantic intent and structural detail.

Multi-Reference Video Editing. Table 3 presents results on TIDE-Bench. TIDE achieves the best overall score among open-source methods and is competitive with closed-source systems. Notably, VINO exhibits a significant drop in Reference Faithfulness under our evaluation protocol, which penalizes copy-pasting reference content without meaningful editing; this reveals that VINO tends to directly replicate reference images rather than performing genuine multi-reference editing. In contrast, TIDE maintains balanced performance across all dimensions, demonstrating stronger multi-reference editing capability.

Subject-to-Video Generation. As shown in Table 4, TIDE achieves the highest Total score among all methods, demonstrating that the unified framework does not compromise generation quality. TIDE leads in Aesthetics and Naturalness while maintaining competitive motion and alignment scores, indicating that multi-task training provides complementary supervision that benefits generation fidelity.

4.3 Qualitative Results

Instruction-Based Video Editing. Figure 3 compares TIDE with Ditto and VINO on three OpenVE-Bench cases spanning object addition, background replacement, and subject replacement. Ditto primarily adjusts the stylistic appearance of the source video rather than executing the intended structural edits. VINO modifies the original video content but introduces unintended alterations to regions that should remain unchanged. In contrast, TIDE performs precise, localized edits that faithfully follow the instruction while preserving the integrity of unedited regions.

Multi-Reference Video Editing. Figure 5 presents two TIDE-Bench cases, each requiring multiple simultaneous editing operations guided by distinct reference images. VINO lacks independent

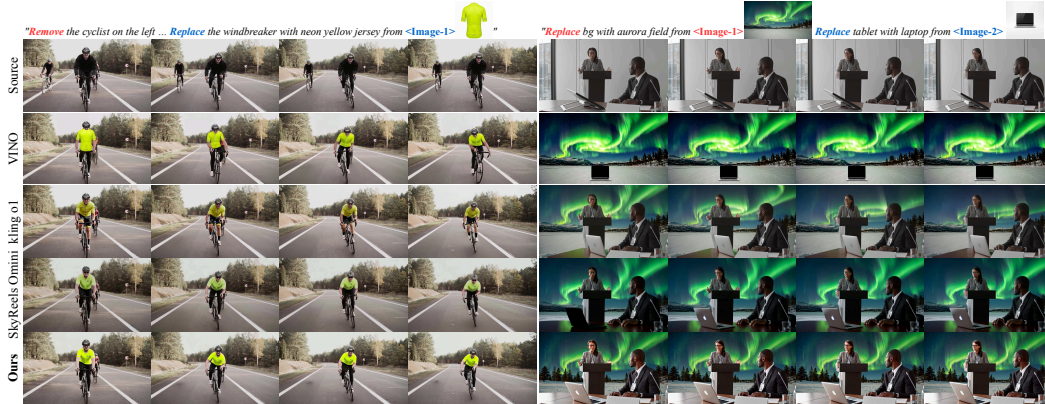


Figure 5: **Qualitative comparison** on TIDE-Bench.

Table 4: Comparison with SOTA methods on OpenS2V.

Method	Total \uparrow	Aes \uparrow	MSmooth \uparrow	MAmp \uparrow	GME \uparrow	Nexus \uparrow	Natural \uparrow
<i>Closed-source</i>							
Kling 1.6 Team et al. (2025b)	60.26	44.59	86.93	41.60	66.20	45.89	74.59
Pika 2.1 Pika Labs (2025)	57.25	46.88	87.06	24.71	69.19	45.40	63.32
Vidu 2.0 Shengshu Technology (2025)	56.16	41.48	90.45	13.52	67.57	43.37	65.88
<i>Open-source</i>							
MAGREF Deng et al. (2025)	57.94	45.02	93.17	21.81	70.47	43.04	66.90
Phantom-1.3B Liu et al. (2025)	56.47	46.67	93.30	14.29	69.43	42.48	62.50
Phantom-14B Liu et al. (2025)	58.10	46.39	<u>96.31</u>	33.42	70.65	37.43	69.35
SkyReels-A2 Chen et al. (2025a)	53.83	39.41	<u>87.93</u>	<u>25.60</u>	64.54	43.75	60.32
VACE-1.3B Jiang et al. (2025)	57.21	<u>48.24</u>	97.20	18.83	<u>71.26</u>	37.91	65.46
VACE-14B Jiang et al. (2025)	58.16	47.21	94.97	15.02	67.27	<u>44.08</u>	67.04
VACE-P1.3B Jiang et al. (2025)	57.08	47.34	96.80	12.03	71.38	40.19	64.31
VINO Chen et al. (2026b)	<u>59.31</u>	45.92	94.73	12.30	69.69	42.67	<u>71.99</u>
TIDE (Ours)	62.62	49.53	95.84	22.56	70.09	49.40	73.66

conditioning control over each reference, resulting in either superficial edits or crude copy-pasting of reference content without proper scene integration. Compared with closed-source methods Kling-O1 and SkyReels-Omni, TIDE achieves comparable or superior multi-reference editing quality while better preserving fine-grained scene details; notably, in the second case, TIDE correctly retains the table on the left side of the scene that other methods fail to preserve.

Subject-to-Video Generation. Figure 4 compares TIDE with HunyuanCustom, VACE-14B, and VINO on multi-reference generation from OpenS2V. HunyuanCustom suffers from entangled reference feature encoding, producing subjects with mixed identities. VACE-14B fails to faithfully follow the text prompt and introduces physically implausible content changes. VINO also deviates from the specified instructions, generating content inconsistent with the prompt. Moreover, all three baselines exhibit poor identity preservation, where the generated subjects fail to maintain visual consistency with the corresponding reference images. TIDE demonstrates strong prompt adherence while accurately preserving the distinct visual identity of each reference subject throughout the generated video. Additional results are in Appendix G.

4.4 Ablation Studies

We ablate TIDE’s core design choices on TIDE-Bench and OpenVE-Bench.

Task Embedding. We evaluate four degraded per-token task embedding configurations (Table 6 in Appendix B). All variants cause substantial degradation, with Reference Faithfulness most affected, confirming that per-token task embeddings are critical for multi-reference identity disambiguation.

Component Ablation. Table 5 (top) shows training-matched variants. Removing the VLM path causes the largest drop on both benchmarks, confirming that VLM-based semantic understanding is essential for interpreting complex editing instructions. Removing VLM encoding for the source video (*w/o VLM-Source*) retains partial performance, suggesting that VLM-based scene understanding

Table 5: Ablation study on components and progressive training.

Method	TIDE-Bench \uparrow	OpenVE \uparrow
w/o VLM	2.56	1.98
w/o VLM-Source	2.89	2.01
Stage 1	2.51	2.99
Stage 2	3.30	2.84
TIDE (Stage 3)	3.41	2.91

of the source provides complementary guidance beyond reference-side features alone. Qualitative comparisons in Appendix A further illustrate these effects.

Progressive Training. Table 5 (bottom) tracks per-stage performance. Stage 2 introduces multi-task data and yields a large gain on TIDE-Bench (+0.79), while Stage 3 adds a further +0.11. On OpenVE-Bench, Stage 1 scores highest (2.99) as it specializes in instruction editing; Stages 2/3 trade a small decrease (−0.15) for substantially improved multi-reference capability (see Appendix A).

Guidance Scale. Figure 6 shows the effect of s_{cfg} on both benchmarks. Performance is robust across $s_{\text{cfg}} \in [3.0, 8.0]$, with $s_{\text{cfg}}=4.0$ achieving the best overall trade-off: it attains the highest OpenVE-Bench score (2.91) while maintaining strong TIDE-Bench performance (3.41). Lower scales ($s_{\text{cfg}}=3.0$) slightly favor multi-reference editing at the expense of instruction compliance, while higher scales ($s_{\text{cfg}} \geq 6.0$) degrade both metrics. We adopt $s_{\text{cfg}}=4.0$ for all main experiments.

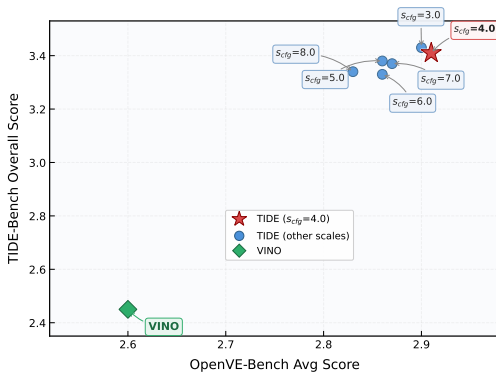


Figure 6: Effect of CFG scale s_{cfg} on OpenVE-Bench and TIDE-Bench. Star marks $s_{\text{cfg}}=4.0$.

5 Conclusion

We presented TIDE, a unified framework that integrates instruction-based video editing, reference-guided video editing, and multi-reference video generation through a joint Diffusion Transformer and vision-language model architecture, equipped with per-token task embeddings and dual-path conditioning. Experiments on OpenVE-Bench, TIDE-Bench, and OpenS2V demonstrate state-of-the-art performance across both editing and generation tasks.

Limitations. Despite strong overall performance, several limitations remain. First, our training data lacks multi-shot editing sequences, limiting TIDE’s ability to perform coherent edits across scene transitions and camera cuts; collecting or synthesizing multi-shot editing data would strengthen this capability. Second, TIDE currently operates exclusively in the visual domain and does not support audio-aware editing (e.g., synchronizing speech or sound effects with visual modifications), an increasingly important direction as audio-visual generation models mature HaCohen et al. (2026); Low et al. (2025). Future work will explore extending the task embedding framework to accommodate multi-shot and audio-visual editing scenarios.

References

Qingyan Bai, Qiuyu Wang, Hao Ouyang, Yue Yu, Hanlin Wang, Wen Wang, Ka Leong Cheng, Shuailei Ma, Yanhong Zeng, Zichen Liu, and 1 others. 2025a. Scaling instruction-based video

- editing with a high-quality synthetic dataset. *arXiv preprint arXiv:2510.15742*.
- Shuai Bai, Yuxuan Cai, Ruizhe Chen, Keqin Chen, and 1 others. 2025b. Qwen3-vl technical report. *arXiv preprint arXiv:2511.21631*.
- Andreas Blattmann, Tim Dockhorn, Sumith Kulal, Daniel Mendelevitch, Maciej Kilian, Dominik Lorenz, Yam Levi, Zion English, Vikram Voleti, Adam Letts, Varun Jampani, and Robin Rombach. 2023. Stable video diffusion: Scaling latent video diffusion models to large datasets. *arXiv preprint arXiv:2311.15127*.
- Tim Brooks, Bill Peebles, Connor Holmes, Will DePue, Yufei Guo, Li Jing, David Schnurr, Joe Taylor, Troy Luhman, Eric Luhman, Clarence Ng, Ricky Wang, and Aditya Ramesh. 2024. Video generation models as world simulators. <https://openai.com/index/video-generation-models-as-world-simulators/>.
- Yuanhao Cai, He Zhang, Xi Chen, Jinbo Xing, Yiwei Hu, Yuqian Zhou, Kai Zhang, Zhifei Zhang, Soo Ye Kim, Tianyu Wang, Yulun Zhang, Xiaokang Yang, Zhe Lin, and Alan Yuille. 2025. Omnivcus: Feedforward subject-driven video customization with multimodal control conditions. *arXiv preprint arXiv:2506.23361*.
- Guibin Chen, Dixuan Lin, Jiangping Yang, Chunze Lin, Junchen Zhu, Mingyuan Fan, Hao Zhang, Sheng Chen, Zheng Chen, Chengcheng Ma, and 1 others. 2025a. Skyreels-v2: Infinite-length film generative model. *arXiv preprint arXiv:2504.13074*.
- Guibin Chen, Dixuan Lin, Jiangping Yang, Youqiang Zhang, Zhengcong Fei, Debang Li, Sheng Chen, Chaofeng Ao, Nuo Pang, Yiming Wang, and 1 others. 2026a. Skyreels-v4: Multi-modal video-audio generation, inpainting and editing model. *arXiv preprint arXiv:2602.21818*.
- Junyi Chen, Tong He, Zhoujie Fu, Pengfei Wan, Kun Gai, and Weicai Ye. 2026b. VINO: A unified visual generator with interleaved omnimodal context. *arXiv preprint arXiv:2601.02358*.
- Tsai-Shien Chen, Aliaksandr Siarohin, Willi Menapace, Yuwei Fang, Kwot Sin Lee, Hung-Yu Tseng, Wei-Sheng Liao, Konstantinos G Derpanis, Sergey Tulyakov, and Jian Ren Wang. 2025b. Multi-subject open-set personalization in video generation. *arXiv preprint arXiv:2501.06187*.
- Xi Chen, Zhifei Zhang, He Zhang, Yuqian Zhou, Soo Ye Kim, Qing Liu, Yijun Li, Jianming Zhang, Nanxuan Zhao, Yilin Wang, Hui Ding, Zhe Lin, and Hengshuang Zhao. 2024. Unireal: Universal image generation and editing via learning real-world dynamics. *arXiv preprint arXiv:2412.07774*.
- Jiaxin Cheng, Tianjun Xiao, and Tong He. 2023. Consistent video-to-video transfer using synthetic dataset. *arXiv preprint arXiv:2311.00213*.
- Gheorghe Comanici, Eric Bieber, Mike Schaekermann, Ice Pasupat, Noveen Sachdeva, Inderjit Dhillon, Marcel Blistein, Ori Ram, Dan Zhang, Evan Rosen, and 1 others. 2025. Gemini 2.5: Pushing the frontier with advanced reasoning, multimodality, long context, and next generation agentic capabilities. *arXiv preprint arXiv:2507.06261*.
- Google DeepMind. 2026. Gemini 3.1 flash-lite. <https://ai.google.dev/>. Accessed: 2026-03-15.
- Yufan Deng, Xun Guo, Yuanyang Yin, Jacob Zhiyuan Fang, Yiding Yang, Yizhi Wang, Shenghai Yuan, Angtian Wang, Bo Liu, Haibin Huang, and 1 others. 2025. Magref: Masked guidance for any-reference video generation. *arXiv preprint arXiv:2505.23742*.
- Zhengcong Fei, Debang Li, Di Qiu, Jiahua Wang, Yikun Dou, Junge Wang, and Mingyuan Fan. 2025. Skyreels-a2: Compose anything in video diffusion transformers. *arXiv preprint arXiv:2504.02436*.
- Michal Geyer, Omer Bar-Tal, Shai Bagon, and Tali Dekel. 2023. Tokenflow: Consistent diffusion features for consistent video editing. *arXiv preprint arXiv:2307.10373*.
- Sharath Girish, Viacheslav Ivanov, Tsai-Shien Chen, Hao Chen, Aliaksandr Siarohin, and Sergey Tulyakov. 2025. Alchemint: Fine-grained temporal control for multi-reference consistent video generation. *arXiv preprint arXiv:2512.10943*.

- Xu Guo, Fulong Ye, Qichao Sun, Liyang Chen, Bingchuan Li, Pengze Zhang, Jiawei Liu, Songtao Zhao, Qian He, and Xiangwang Hou. 2026. Dreamid-omni: Unified framework for controllable human-centric audio-video generation. *arXiv preprint arXiv:2602.12160*.
- Yuwei Guo, Ceyuan Yang, Anyi Rao, Zhengyang Liang, Yaohui Wang, Yu Qiao, Maneesh Agrawala, Dahua Lin, and Bo Dai. 2023. Animatediff: Animate your personalized text-to-image diffusion models without specific tuning. *arXiv preprint arXiv:2307.04725*.
- Yoav HaCohen, Benny Brazowski, Nisan Chiprut, Yaki Bitterman, Andrew Kvochko, Avishai Berkowitz, Daniel Shalem, Daphna Lifschitz, Dudu Moshe, Eitan Porat, and 1 others. 2026. Ltx-2: Efficient joint audio-visual foundation model. *arXiv preprint arXiv:2601.03233*.
- Haoyang He, Jie Wang, Jiangning Zhang, Zhucun Xue, Xingyuan Bu, Qiangpeng Yang, Shilei Wen, and Lei Xie. 2025a. Openve-3m: A large-scale high-quality dataset for instruction-guided video editing. *arXiv preprint arXiv:2512.07826*.
- Xuanhua He, Quande Liu, Zixuan Ye, Weicai Ye, Qiulin Wang, Xintao Wang, Qifeng Chen, Pengfei Wan, Di Zhang, and Kun Gai. 2025b. Fulldit2: Efficient in-context conditioning for video diffusion transformers. *arXiv preprint arXiv:2506.04213*.
- Jonathan Ho, Tim Salimans, Alexey Gritsenko, William Chan, Mohammad Norouzi, and David J. Fleet. 2022. Video diffusion models. *Advances in Neural Information Processing Systems*, 35.
- Susung Hong. 2024. Smoothed energy guidance: Guiding diffusion models with reduced energy curvature of attention. *arXiv preprint arXiv:2408.00760*.
- Teng Hu, Zhentao Yu, Zhengguang Zhou, Sen Liang, Yuan Zhou, Qin Lin, and Qinglin Lu. 2025. Hunyuancustom: A multimodal-driven architecture for customized video generation. *arXiv preprint arXiv:2505.04512*.
- Yuzhou Huang, Ziyang Yuan, Quande Liu, Qiulin Wang, Xintao Wang, Ruimao Zhang, Pengfei Wan, Di Zhang, and Kun Gai. 2025. Conceptmaster: Multi-concept video customization on diffusion transformer models without test-time tuning. *arXiv preprint arXiv:2501.04698*.
- Zeyinzi Jiang, Zhen Han, Chaojie Mao, Jingfeng Zhang, Yulin Pan, and Yu Liu. 2025. Vace: All-in-one video creation and editing. *arXiv preprint arXiv:2503.07598*.
- Ozgur Kara, Bariscan Kurtkaya, Hidir Yesiltepe, James M Rehg, and Pinar Yanardag. 2024. Rave: Randomized noise shuffling for fast and consistent video editing with diffusion models. In *Proceedings of the IEEE/CVF Conference on Computer Vision and Pattern Recognition*, pages 6507–6516.
- Weijie Kong, Qi Tian, Zijian Zhang, Rox Min, Zuozhuo Dai, Jin Zhou, Jiangfeng Xiong, Xin Li, Bo Wu, Jianwei Zhang, and 1 others. 2024. Hunyuanvideo: A systematic framework for large video generative models. *arXiv preprint arXiv:2412.03603*.
- Minghan Li, Chenxi Xie, Yichen Wu, Lei Zhang, and Mengyu Wang. 2025a. Five: A fine-grained video editing benchmark for evaluating emerging diffusion and rectified flow models. *arXiv preprint arXiv:2503.13684*.
- Zhaoyang Li, Dongjun Qian, Kai Su, Qishuai Diao, Xiangyang Xia, Chang Liu, Wenfei Yang, Tianzhu Zhang, and Zehuan Yuan. 2025b. Bindweave: Subject-consistent video generation via cross-modal integration. *arXiv preprint arXiv:2510.00438*.
- Xinyao Liao, Xianfang Zeng, Ziye Song, Zhoujie Fu, Gang Yu, and Guosheng Lin. 2025. In-context learning with unpaired clips for instruction-based video editing. *arXiv preprint arXiv:2510.14648*.
- Yaron Lipman, Ricky TQ Chen, Heli Ben-Hamu, Maximilian Nickel, and Matt Le. 2022. Flow matching for generative modeling. *arXiv preprint arXiv:2210.02747*.
- Jialun Liu, Tian Li, Xiao Cao, Yukuo Ma, Gonghu Shang, Haibin Huang, Chi Zhang, Xiangzhen Chang, Zhiyong Huang, Jiakui Hu, Zuoxin Li, Yuanzhi Liang, Cong Liu, Junqi Liu, Robby T. Tan, Haitong Tang, Qizhen Weng, Yifan Xu, Liying Yang, and 4 others. 2026. Tele-omni: a unified multimodal framework for video generation and editing. *arXiv preprint arXiv:2602.09609*.

- Lijie Liu, Tianxiang Ma, Bingchuan Li, Zhuowei Chen, Jiawei Liu, Gen Li, Siyu Zhou, Qian He, and Xinglong Wu. 2025. Phantom: Subject-consistent video generation via cross-modal alignment. *arXiv preprint arXiv:2502.11079*.
- Chetwin Low, Weimin Wang, and Calder Katyal. 2025. Ovi: Twin backbone cross-modal fusion for audio-video generation. *arXiv preprint arXiv:2510.01284*.
- Xin Ma, Yaohui Wang, Gengyun Jia, Xinyuan Chen, Ziwei Liu, Yuan-Fang Li, Cunjian Chen, and Yu Qiao. 2024. Latte: Latent diffusion transformer for video generation. *arXiv preprint arXiv:2401.03048*.
- William Peebles and Saining Xie. 2022. Scalable diffusion models with transformers. *arXiv preprint arXiv:2212.09748*.
- Pika Labs. 2025. Pika 2.1. <https://pikaddition.com/pika-2-1>.
- Adam Polyak, Amit Zohar, Andrew Brown, Andros Tjandra, Animesh Sinha, Ann Lee, Apoorv Vyas, Bowen Shi, Chih-Yao Ma, Ching-Yao Chuang, and 1 others. 2024. Movie gen: A cast of media foundation models. *arXiv preprint arXiv:2410.13720*.
- Chenyang Qi, Xiaodong Cun, Yong Zhang, Chenyang Lei, Xintao Wang, Ying Shan, and Qifeng Chen. 2023. Fatezero: Fusing attentions for zero-shot text-based video editing. In *Proceedings of the IEEE/CVF International Conference on Computer Vision*, pages 15932–15942.
- Shengshu Technology. 2025. Vidu 2.0. <https://www.vidu.cn/>.
- Uriel Singer, Adam Polyak, Thomas Hayes, Xi Yin, Jie An, Songyang Zhang, Qiyuan Hu, Harry Yang, Oron Ashual, Oran Gafni, Devi Parikh, Sonal Gupta, and Yaniv Taigman. 2022. Make-a-video: Text-to-video generation without text-video data. *arXiv preprint arXiv:2209.14792*.
- Jiaming Song, Chenlin Meng, and Stefano Ermon. 2020. Denoising diffusion implicit models. *arXiv preprint arXiv:2010.02502*.
- Ziyang Song, Xinyu Gong, Bangya Liu, and Zelin Zhao. 2026. Mv-s2v: Multi-view subject-consistent video generation. *arXiv preprint arXiv:2601.17756*.
- Zhiyu Tan, Hao Yang, Luozheng Qin, Jia Gong, Mengping Yang, and Hao Li. 2025. Omni-video: Democratizing unified video understanding and generation. *arXiv preprint arXiv:2507.06119*.
- DecartAI Team. 2025. Lucy edit: Open-weight text-guided video editing.
- Gemma Team, Aishwarya Kamath, Johan Ferret, Shreya Krawczyk, Robert McIlroy, Nate Goodman, Sayed Hadi Hashemi, Noah Fiedel, and 1 others. 2025a. Gemma 3 technical report. *arXiv preprint arXiv:2503.19786*.
- Kling Team, Jialu Chen, Yuanzheng Ci, Xiangyu Du, Zipeng Feng, Kun Gai, Sainan Guo, Feng Han, Jingbin He, Kang He, and 1 others. 2025b. Kling-omni technical report. *arXiv preprint arXiv:2512.16776*.
- Team Wan, Ang Wang, Baole Ai, Bin Wen, Chaojie Mao, Chen-Wei Xie, Di Chen, Fei Wu Yu, Haiming Zhao, Jianxiao Yang, and 1 others. 2025. Wan: Open and advanced large-scale video generative models. *arXiv preprint arXiv:2503.20314*.
- Tong Wang, Meng Zou, Chengjing Wu, Xiaochao Qu, Luoqi Liu, Xiaolin Hu, and Ting Liu. 2026a. Mive: Multiscale vision-language features for reference-guided video editing. *arXiv preprint arXiv:2605.14664*.
- Weicheng Wang, Zhicheng Zhang, Zhongqi Zhang, Juncheng Zhou, Yongjie Zhu, Wenyu Qin, Meng Wang, Pengfei Wan, and Jufeng Yang. 2026b. Live: Leveraging image manipulation priors for instruction-based video editing. *arXiv preprint arXiv:2604.17021*.
- Hongyang Wei, Hongbo Liu, Zidong Wang, Yi Peng, Baixin Xu, Size Wu, Xuying Zhang, Xianglong He, Zexiang Liu, Peiyu Wang, and 1 others. 2026a. Skywork unipic 3.0: Unified multi-image composition via sequence modeling. *arXiv preprint arXiv:2601.15664*.

- Xinyu Wei, Kangrui Cen, Hongyang Wei, Zhen Guo, Bairui Li, Zeqing Wang, Jinrui Zhang, and Lei Zhang. 2026b. Mico-150k: A comprehensive dataset advancing multi-image composition. In *Proceedings of the IEEE/CVF Conference on Computer Vision and Pattern Recognition*, pages 29695–29706.
- Chenfei Wu, Jiahao Li, Jingren Zhou, Junyang Lin, Kaiyuan Gao, Kun Yan, Sheng ming Yin, Shuai Bai, Xiao Xu, Yilei Chen, Yuxiang Chen, Zecheng Tang, Zekai Zhang, Zhengyi Wang, and 1 others. 2025a. Qwen-image technical report. *Preprint*, arXiv:2508.02324.
- Yuhui Wu, Liyi Chen, Ruibin Li, Shihao Wang, Chenxi Xie, and Lei Zhang. 2025b. Insvie-1m: Effective instruction-based video editing with elaborate dataset construction. In *Proceedings of the IEEE/CVF International Conference on Computer Vision*, pages 16692–16701.
- Shitao Xiao, Yueze Wang, Junjie Zhou, Huaying Yuan, Xingrun Xing, Ruiran Yan, Chaofan Li, Shuting Wang, Tiejun Huang, and Zheng Liu. 2024. Omnigen: Unified image generation. *arXiv preprint arXiv:2409.11340*.
- Chunyu Xie, Bin Wang, Fanjing Kong, Jincheng Li, Dawei Liang, Gengshen Zhang, Dawei Leng, and Yuhui Yin. 2025. Fg-clip: Fine-grained visual and textual alignment. *arXiv preprint arXiv:2505.05071*.
- Hao Yang, Zhiyu Tan, Jia Gong, Luo Zheng Qin, Heseng Chen, Xiaomeng Yang, Yuqing Sun, Yuetan Lin, Mengping Yang, and Hao Li. 2026. Omni-video 2: Scaling mllm-conditioned diffusion for unified video generation and editing. *arXiv preprint arXiv:2602.08820*.
- Tao Yang, Ruibin Li, Yangming Shi, Yuqi Zhang, Qide Dong, Haoran Cheng, Weiguo Feng, Shilei Wen, Bingyue Peng, and Lei Zhang. 2025. Many-for-many: Unify the training of multiple video and image generation and manipulation tasks. *arXiv preprint arXiv:2506.01758*.
- Zhuoyi Yang, Jiayan Teng, Wendi Zheng, Ming Ding, Shiyu Huang, Jiazheng Xu, Yuanming Yang, Wenyi Hong, Xiaohan Zhang, Guanyu Feng, and 1 others. 2024. Cogvideox: Text-to-video diffusion models with an expert transformer. *arXiv preprint arXiv:2408.06072*.
- Hu Ye, Jun Zhang, Sibao Liu, Xiao Han, and Wei Yang. 2023. Ip-adapter: Text compatible image prompt adapter for text-to-image diffusion models. *arXiv preprint arXiv:2308.06721*.
- Shoubin Yu, Difan Liu, Ziqiao Ma, Yicong Hong, Yang Zhou, Hao Tan, Joyce Chai, and Mohit Bansal. 2025. Veggie: Instructional editing and reasoning video concepts with grounded generation. *arXiv preprint arXiv:2503.14350*.
- Shenghai Yuan, Xianyi He, Yufan Deng, Yang Ye, Jinfa Huang, Bin Lin, Jiebo Luo, and Li Yuan. 2025. Opens2v-nexus: A detailed benchmark and million-scale dataset for subject-to-video generation. *arXiv preprint arXiv:2505.20292*.
- Zangwei Zheng, Xiangyu Peng, Tianji Yang, Chenhui Shen, Shenggui Li, and Yang You. 2024. Open-sora: Democratizing efficient video production for all. *arXiv preprint arXiv:2412.20404*.
- Yong Zhong, Zhuoyi Yang, Jiayan Teng, Xiaotao Gu, and Chongxuan Li. 2025. Concat-id: Towards universal identity-preserving video synthesis. *arXiv preprint arXiv:2503.14151*.
- Jiahao Zhu, Shanshan Lao, Lijie Liu, Gen Li, Tianhao Qi, Wei Han, Bingchuan Li, Fangfang Liu, Zhuowei Chen, Tianxiang Ma, Qian He, Yi Zhou, and Xiaohua Xie. 2026. Libragen: Playing a balance game in subject-driven video generation. *arXiv preprint arXiv:2603.13506*.
- Bojia Zi, Penghui Ruan, Marco Chen, Xianbiao Qi, Shaozhe Hao, Shihao Zhao, Youze Huang, Bin Liang, Rong Xiao, and Kam-Fai Wong. 2025. Se\~norita-2m: A high-quality instruction-based dataset for general video editing by video specialists. *arXiv preprint arXiv:2502.06734*.

A Qualitative Ablation Analysis

Figure 7 presents a qualitative comparison of ablation variants on an OpenVE-Bench editing case, where the instruction asks to replace a white compact car with a metallic blue electric sports car. *w/o VLM* removes the original black car from the scene entirely rather than performing the intended replacement, failing to interpret the editing instruction correctly. *w/o VLM-Source* successfully replaces the car with a blue vehicle, but the left rear wheel of the replacement car is missing, indicating degraded structural fidelity without VLM-based source scene understanding. Only the full TIDE model correctly generates a complete blue sports car while maintaining temporal consistency and preserving the reporter and background scene.

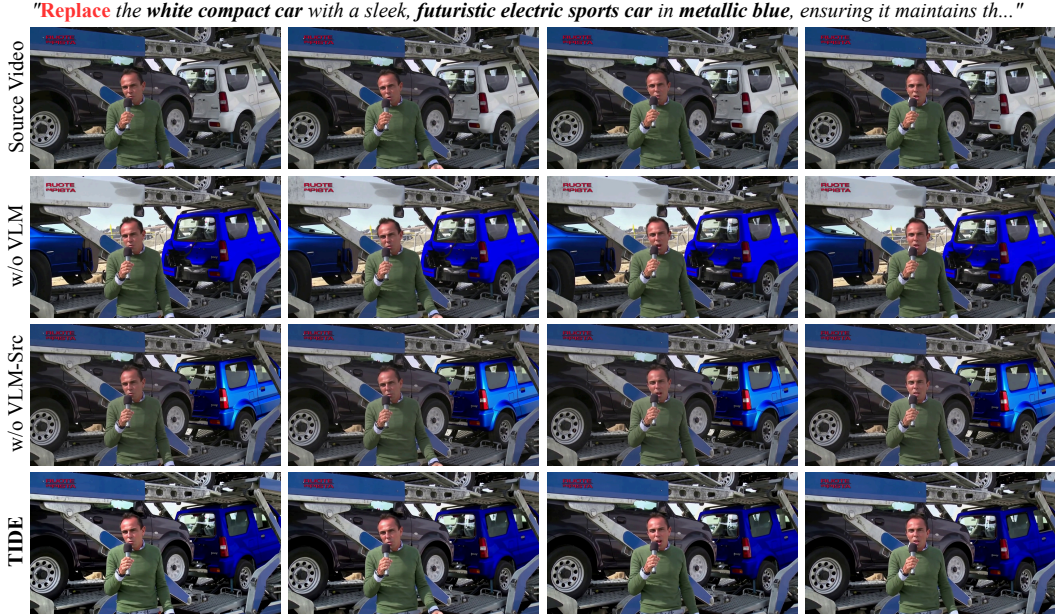


Figure 7: Qualitative ablation on an OpenVE-Bench editing case. Only the full TIDE model faithfully follows the instruction while preserving the scene.

Figure 8 shows a progressive training ablation on a TIDE-Bench style transfer case, where the instruction asks to apply a low-poly 3D geometric art style from a reference image to a source video of a person playing guitar on stairs. Stage 1 (instruction-edit only) applies the low-poly style but also introduces content from the reference image (mountains, river) into the background, failing to disentangle style from content. Stage 2 improves content preservation (the person and guitar are maintained), but the style transfer leaks reference content into the background (cartoon-like sky and buildings visible through the window), and overall stylization is inconsistent. The full TIDE model successfully transfers only the low-poly geometric art style while faithfully preserving the original video content: the person, guitar, stairs, and indoor setting remain intact with consistent stylization across frames, demonstrating that progressive multi-task training is critical for learning to separate style from content in reference-guided editing.

B Task Embedding Ablation

We evaluate four degraded task embedding configurations using the same trained model (Table 6): (a) all reference images share a single $\tau=1$; (b) swapping τ between references and source; (c) assigning an untrained $\tau=99$; (d) all conditioning tokens share $\tau=1$. All variants exhibit substantial degradation on TIDE-Bench, with average scores dropping from 3.41 to 2.09–2.35. Reference Faithfulness is the most affected dimension (3.44 \rightarrow 1.84–2.26), indicating that per-token task embeddings are critical for distinguishing and preserving multiple reference identities. Variant (c) performs worst, suggesting that the learned embedding directions carry task-specific semantics beyond mere token differentiation.

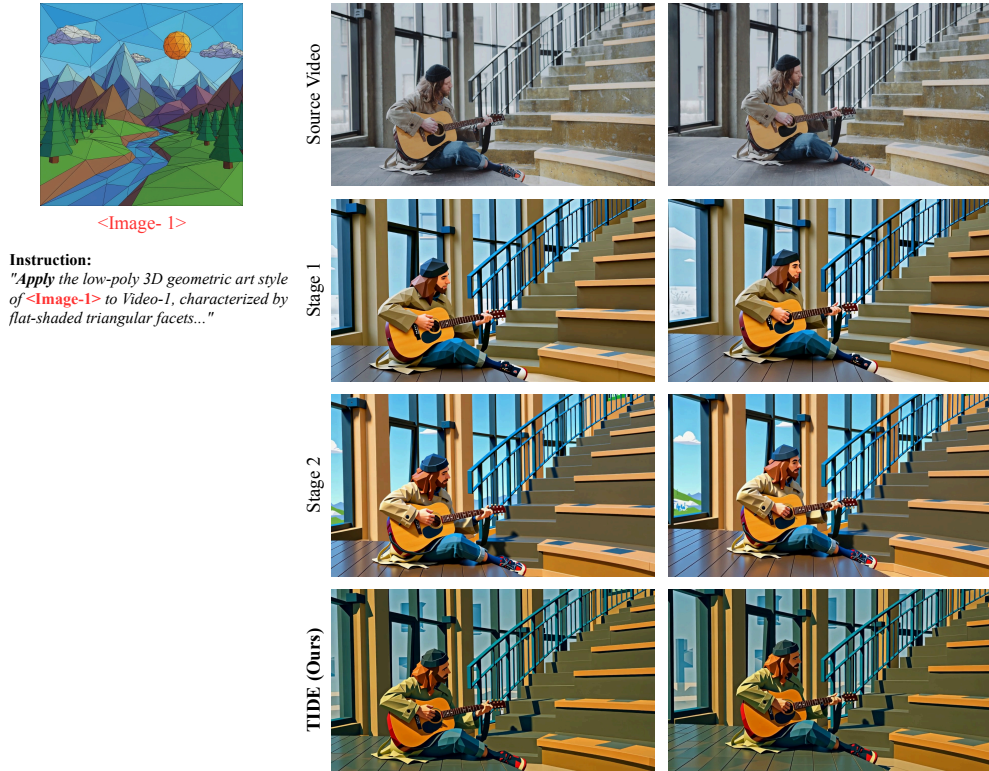


Figure 8: Progressive training ablation on a TIDE-Bench style transfer case. Stage 1 conflates reference content with style; Stage 2 partially leaks; TIDE (Full) transfers only the style.

Table 6: Task embedding ablation on TIDE-Bench.

Variant	Edit \uparrow	Ref \uparrow	V&T \uparrow	Pres \uparrow	Qual \uparrow	Avg. \uparrow
(a) All refs share $\tau=1$	2.77	1.98	2.30	2.23	2.19	2.29
(b) Swap τ (ref \leftrightarrow src)	2.76	2.05	2.30	2.28	2.20	2.32
(c) Untrained $\tau=99$	2.45	1.84	2.07	2.05	2.03	2.09
(d) All cond share $\tau=1$	2.80	2.26	2.29	2.22	2.17	2.35
TIDE (Full)	4.07	3.44	3.20	3.21	3.15	3.41

C TIDE-Bench Details

Benchmark Construction. TIDE-Bench is a multi-reference video editing benchmark designed to evaluate the ability to combine reference-guided editing with instruction-following. Each sample contains: (1) a source video, (2) 1 – 4 reference images depicting target subjects, styles, or objects, and (3) a text instruction describing the desired editing operation. Samples span diverse editing types: style transfer with reference (28%), object replacement with reference (25%), subject insertion (22%), multi-subject composition (15%), and attribute transfer (10%). Source videos are collected from publicly available datasets and filtered for diversity in scene type, motion, and complexity.

Evaluation Protocol. We adopt the LLM-as-judge paradigm and use Gemini-3.1-Pro Comanici et al. (2025) as the automated evaluator. Each generated video is scored on five dimensions using edit-type-specific prompts: global style transfer cases use the prompt in Prompt 1, while all local editing cases (addition, removal, replacement, background change, and their combinations) use the prompt in Prompt 2. The evaluator receives the original video, all reference images with role descriptions, the editing instruction, and the edited video. Reference Faithfulness is scored per-reference (Ref-1,

Ref-2, ...) and aggregated via \min to reflect worst-case reference fidelity. To prevent inflated scores from naive copy-pasting of reference content without meaningful editing, the evaluation enforces the constraint that Reference Faithfulness, Visual & Temporal Quality, Scene Preservation, and Overall Quality must all be \leq Edit Completeness. This penalises methods that achieve high reference fidelity by simply overlaying reference images onto the video without proper scene integration. The Overall score is computed as the average of the five dimensions. We plan to publicly release the benchmark data and evaluation code upon acceptance.

Prompt 1: TIDE-Bench: Global Style Transfer Evaluation

You are an expert evaluator for video style transfer editing. You will be provided with three visual inputs in order:

1. **[Original Video]**: The source video before any editing.
2. **[Reference Image-1]**: A style reference image that defines the target artistic style.
3. **[Edited Video]**: The result after applying the style transfer.

Editing instruction: {instruction}

Evaluate on five dimensions, each on a 1–5 integer scale:

Edit Completeness (Style Fidelity)

Assess whether the target artistic style has been fully and consistently applied across the entire video duration. 5 = Full, faithful transfer: colour palette, texture, brushwork/artistic techniques match the style reference consistently over every frame of the entire video. 4 = Style reproduced well across almost the whole video; only small local regions or brief temporal moments show mismatches. 3 = Key style traits (e.g., colour palette or texture) are present but application is patchy, inconsistent across frames, or fades in/out. 2 = Style shows in only a few areas or frames; rest of the video retains original appearance or shows unrelated styles. 1 = Target style is absent, barely detectable, or a completely wrong style was applied.

Reference Faithfulness

Score EACH reference image independently on a 1–5 scale. Compare the edited video’s visual style against the reference image:

5 = Style characteristics (colour palette, texture patterns, brushwork, artistic technique) exactly match the reference image throughout the video. 4 = Strong resemblance to reference style; the artistic approach is clearly the same, only fine details or subtle tonal differences. 3 = General style direction is correct (e.g., right artistic movement) but noticeable differences in palette, texture density, or technique. 2 = Vaguely related style but substantially different from the reference (wrong colour scheme, different texture, or inconsistent technique). 1 = No discernible resemblance to the reference style image at all.

Visual & Temporal Quality

Assess the visual fidelity and temporal stability of the edited video. Pay attention to flickering, boiling textures, edge artifacts, and frame-to-frame consistency.

5 = Perfectly stable and temporally coherent; no flickering, clean edges, high resolution maintained throughout. 4 = Largely stable with only minor, subtle flickering in areas of complex motion; quality is high. 3 = Noticeable but tolerable flicker or texture “boiling”, especially during fast motion or scene transitions. 2 = Significant and distracting flickering, jittering, or temporal inconsistency that degrades viewing experience. 1 = Extreme flickering or “boiling” effects; video is essentially unwatchable.

Scene Preservation (Content Preservation)

Assess whether the original video’s content (objects, spatial layout, motion trajectories, perspective) is preserved. Only stylistic changes should be made.

5 = All objects, spatial relations, and motion perfectly kept; only stylistic changes applied. 4 = Nearly all geometry and motion intact; only slight, non-distracting deformation in minor areas. 3 = Overall structure and motion direction correct; some local warping, slight motion jerkiness, or minor spatial distortion. 2 = Main subject recognisable, but size, perspective, motion speed, or key body parts are clearly wrong. 1 = Major objects, layout, or overall motion lost/distorted; scene is barely recognisable as the original.

Overall Quality

Holistic assessment of the final video’s quality as a creative output.

5 = Publication-ready; aesthetically pleasing, high resolution, physically plausible, no visible artifacts. 4 = Good quality; minor imperfections only visible on close inspection. 3 = Acceptable quality; some noticeable artifacts or quality issues but still viewable. 2 = Poor quality; obvious artifacts, blur, or distortion that significantly degrade the result. 1 = Very poor; heavily degraded, unwatchable.

Rules: Reference Faithfulness, Visual & Temporal Quality, Scene Preservation, and Overall Quality scores must ALL be \leq Edit Completeness score.

Response Format:

Brief reasoning: <one sentence, max 30 words>

Edit Completeness: <1–5>

Reference Faithfulness: Ref-1=<1–5> (one score per reference image)
Visual & Temporal Quality: <1–5>
Scene Preservation: <1–5>
Overall Quality: <1–5>

Prompt 2: TIDE-Bench: Local / Multi-Reference Editing Evaluation

You are an expert evaluator for multi-reference video editing. You will be provided with visual inputs in order:

1. **[Original Video]**: The source video before any editing.
2. **[Reference Image-1], [Reference Image-2], ...**: Reference images defining what should be added, replaced, or used as background.
3. **[Edited Video]**: The result after applying the editing operations.

Editing instruction: {instruction}

Edit type: {edit_type_desc}

Evaluate on five dimensions, each on a 1–5 integer scale:

Edit Completeness (Prompt Compliance)

Assess whether ALL requested editing operations were actually performed correctly and consistently throughout the video duration. Consider both whether each operation happened and whether it targeted the correct subjects.

5 = Every requested operation fully executed with correct targets, maintained consistently for the entire video duration. 4 = All operations attempted and mostly successful; one minor deficiency (e.g., slight inconsistency in a few frames). 3 = At least one operation is only partially done, inconsistently applied, or missing from some frames. 2 = Multiple operations missing, only superficially executed, or applied to wrong targets. 1 = No discernible editing performed, or an entirely wrong/unrelated edit was applied.

Reference Faithfulness

Score EACH reference image independently on a 1–5 scale. For each reference, assess how faithfully its visual content (shape, colour, texture, identity-defining features) was reproduced in the edited video:

5 = Shape, colour, texture, and distinctive features exactly match the reference; the element is immediately recognisable as the same object/scene. 4 = Strong resemblance; correct category and key attributes preserved; only fine details (e.g., minor texture, exact proportions) differ. 3 = Correct category but noticeable drift (wrong shade/colour, simplified geometry, missing distinctive features). 2 = A vaguely related element appears but is substantially different from the reference in shape, colour, or identity. 1 = Referenced content is completely absent from the edited video, or an entirely unrelated element was used.

Visual & Temporal Quality

Assess the visual fidelity and temporal stability of the edited video. Focus on the edit regions but also check for artifacts introduced elsewhere. Pay attention to flickering, edge seams, colour bleeding, and frame-to-frame consistency.

5 = Perfectly seamless integration; edit area is undetectable, no flicker, jitter, or quality degradation anywhere. 4 = Style and quality almost uniform and stable; tiny temporal artefacts visible only on frame-by-frame inspection. 3 = Basic quality acceptable but noticeable issues: lighting/palette clashes, inconsistent across frames, minor flickering in edit regions. 2 = Obvious seams/edges around edited areas, strong colour mismatch with surroundings, significant flickering or jittering. 1 = Video heavily broken, massive distortion, or uncontrollable flicker; edit regions are clearly artificial.

Scene Preservation (Physical Coherence)

Assess whether regions that should NOT be edited remain unchanged, and whether the overall physical plausibility (motion, lighting, shadows, perspective) is maintained.

5 = Unedited regions are pixel-faithful to original; motion, lighting, shadows, perspective all physically correct and temporally stable. 4 = Visually identical to original under casual viewing; only subtle deformation detectable on close inspection in non-edit areas. 3 = Most of the scene preserved but noticeable artifacts in untargeted areas; minor physics errors (wrong shadows, slight perspective shift). 2 = Significant unintended changes: subject deformation, objects vanishing, wrong shadows, or spatial layout altered. 1 = Original content largely destroyed or unrecognisable; massive unintended modifications throughout.

Overall Quality

Holistic assessment of the final video as a creative output, considering aesthetic appeal, resolution, and freedom from artifacts.

5 = Publication-ready; aesthetically pleasing, high resolution, physically plausible, no visible artifacts. 4 = Good quality overall; minor imperfections only visible on close inspection. 3 = Acceptable quality; some noticeable artifacts, blur, or quality issues but still viewable. 2 = Poor quality; obvious artifacts, distortion, or degradation that significantly degrade the result. 1 = Very poor; heavily degraded, unwatchable.

Rules: Reference Faithfulness, Visual & Temporal Quality, Scene Preservation, and Overall Quality scores must ALL be \leq Edit Completeness score. If the reference content appears as a crude overlay or copy-paste with poor scene integration, the Reference Faithfulness score must be penalised accordingly (capped at the Edit Completeness score). If no reference images are provided, skip Reference Faithfulness and write “N/A”.

Response Format:

Brief reasoning: <one sentence, max 30 words>

Edit Completeness: <1–5>

Reference Faithfulness: Ref-1=<1–5>, Ref-2=<1–5>, ... (one score per reference; if no refs, write N/A)

Visual & Temporal Quality: <1–5>

Scene Preservation: <1–5>

Overall Quality: <1–5>

D Training Data and Stage Configuration

Training Data. Our training pool comprises $\sim 1.80\text{M}$ samples organized into five categories: (i) *Reference-guided video editing* ($\sim 700\text{K}$): self-constructed data covering addition, removal, replacement, and style-reference editing, of which $\sim 30\text{K}$ are multi-reference editing samples with 2–4 references (construction details in Appendix E); (ii) *Instruction-based video editing* ($\sim 500\text{K}$): source-target video pairs with editing instructions from Ditto Bai et al. (2025a) and OpenVE He et al. (2025a); (iii) *Image editing* ($\sim 170\text{K}$): multi-reference image editing data from MICo Wei et al. (2026b) and Unipic Wei et al. (2026a), treated as single-frame video; (iv) *Subject-to-video generation* ($\sim 330\text{K}$): text-subject-to-video data with cross-video identity pairing (Appendix F); (v) *Reference-guided style video editing* ($\sim 100\text{K}$): style-level reference-conditioned video editing pairs.

Progressive Stage Configuration. Training proceeds through three stages with increasing task complexity. Stage 1 ($\sim 3\text{K}$ steps, $\text{lr} = 1 \times 10^{-4}$) trains exclusively on instruction-based editing data (categories iii, iv) to establish basic editing capability. Stage 2 ($\sim 7\text{K}$ steps, $\text{lr} = 5 \times 10^{-5}$) introduces the full multi-task mixture, adding reference-guided editing (i, ii), multi-reference editing (v, vi), and subject-to-video generation (vii, viii). Stage 3 ($\sim 10\text{K}$ steps, $\text{lr} = 2 \times 10^{-5}$) continues multi-task training with refined sampling ratios that up-weight underrepresented categories (vi, viii) for long-horizon convergence. All step counts are normalized to 32 GPUs with gradient accumulation of 4 (effective batch size 128). The data composition ratios across the three stages are illustrated in Figure 9.

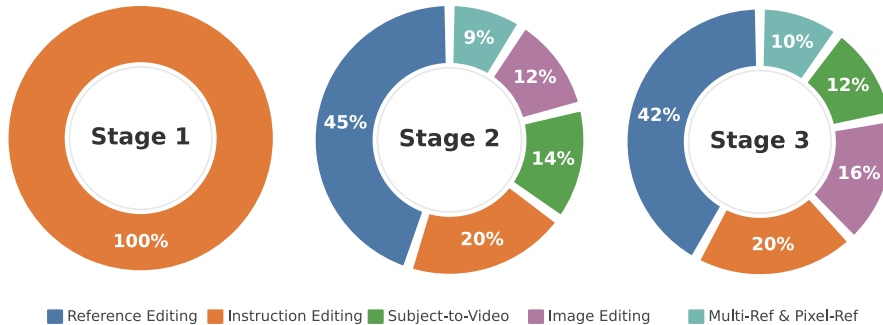


Figure 9: Data composition ratios across the three progressive training stages. Stage 1 uses only instruction-based editing data; Stage 2 introduces the full multi-task mixture; Stage 3 refines sampling ratios to balance underrepresented categories.

E Reference-Guided Editing Data Construction

We construct large-scale reference-guided video editing data from existing open-source instruction-based editing datasets (OpenVE-3M He et al. (2025a) and Ditto Bai et al. (2025a)) through an automated extraction-and-filtering pipeline. Starting from the available (source video, target video, instruction) triplets, our goal is to obtain (source video, target video, reference image, instruction)

quadruplets. The pipeline operates in two phases: *single-reference extraction* converts instruction-edit video pairs into reference-guided quadruplets, and *multi-reference extension* constructs multi-reference training samples through iterative editing.

Single-Reference Extraction. Given a (source video, target video, instruction) triplet from the instruction-based editing datasets, the pipeline proceeds through four stages:

1. **First-Frame Extraction.** We extract the first frame from both the source video and the target video, producing a source frame and a target frame that capture the visual difference introduced by the edit.
2. **Reference Prompt Generation.** A VLM (Gemini DeepMind (2026)) takes the source frame, target frame, and the original editing instruction as input to generate a descriptive prompt for extracting a clean reference image. The generated prompt describes the visual element that should be isolated as the reference (e.g., the added object, the replacement subject, or the target style).
3. **Reference Image Extraction.** The source frame, target frame, and the generated reference prompt are fed into Qwen Image Edit Wu et al. (2025a) to extract a clean, isolated reference image. This produces a reference image that depicts the target visual element without extraneous background or context, completing the quadruplet (source video, target video, reference image, instruction).
4. **Quality Filtering.** A VLM-based filter (Gemini) evaluates each quadruplet on reference image clarity, reference-edit consistency, and instruction accuracy. Samples falling below quality thresholds are removed. This yields $\sim 700\text{K}$ single-reference editing quadruplets spanning diverse edit types including addition, replacement, background change, removal, and style transfer.

Multi-Reference Extension. Multi-reference editing data is constructed by performing two rounds of instruction-based editing. Starting from the single-reference editing quadruplets produced above, we apply an additional instruction-based edit to obtain a second editing layer, which enables extracting a second reference image:

1. **Second-Round Instruction Editing.** Given a single-reference quadruplet (source video V_s , target video V_t , reference image I_1 , instruction c_1), we apply a new instruction-based edit to V_t , producing a further-edited video $V_{t'}$ with a new editing instruction c_2 .
2. **Second Reference Extraction.** The newly edited video $V_{t'}$ and the previous target video V_t now form a new (source, target) pair. We apply the same single-reference extraction pipeline described above (first-frame extraction, Gemini-based reference prompt generation, and Qwen Image Edit-based reference extraction) to obtain a second reference image I_2 .
3. **Multi-Reference Assembly.** This produces a multi-reference editing sample: (source video V_s , final target video $V_{t'}$, reference images $\{I_1, I_2\}$, composite instruction).
4. **Quality Filtering.** A VLM-based quality filter removes samples with artifacts, inconsistent references, or conflicting edits. This produces $\sim 30\text{K}$ multi-reference video editing samples.

F Subject-to-Video Data Construction

We construct subject-to-video (S2V) training data from large-scale internal video collections through an automated subject detection, clustering, and pairing pipeline. The goal is to produce training tuples of (reference subject image, target video, caption) where the reference subject appears in a different video than the target, preventing trivial copy-paste solutions.

The pipeline proceeds through six stages:

1. **Frame Sampling.** We uniformly sample 10+ keyframes from each video clip in the source collection ($\sim 1\text{M}$ clips).
2. **Per-Frame Subject Detection.** Qwen3-VL-8B Bai et al. (2025b) performs open-vocabulary subject detection on each sampled frame, producing bounding boxes and confidence scores for all detected subjects (persons, animals, objects). Low-confidence detections (< 0.09) are discarded.
3. **Subject Cropping & Embedding.** Each detected subject is cropped from its frame and encoded into a 768-dimensional identity embedding using FG-CLIP Xie et al. (2025), a fine-grained visual encoder optimized for subject identity representation.
4. **Cross-Video Identity Clustering.** Subject embeddings are clustered using K-means with cosine similarity to group instances of the same identity across different video clips. An additional Qwen-VL-based identity verification step filters false positives from the clusters.

5. **Quality Filtering.** We apply multi-dimensional filtering to remove low-quality subject images: blur detection (Laplacian variance and learned blur scores), text overlay detection, occlusion detection, face/body consistency checks, and aesthetic scoring. Only subjects passing all quality gates are retained.
6. **Caption Generation & Formatting.** For each valid subject-video pair, a VLM (Gemini / Qwen-VL) generates a subject-driven caption in the format “Based on the [subject] in Image-1, generate a video where...,” explicitly referencing the subject image. The final output is formatted as (reference image, target video, subject-conditioned caption) training tuples.

A key design choice is *cross-video pairing*: the reference image is always drawn from a different video clip than the target. This ensures the model cannot learn to trivially copy the reference into the target and must instead learn genuine identity-preserving generation. The pipeline produces $\sim 225\text{K}$ single-reference S2V pairs. An additional $\sim 10\text{K}$ high-quality multi-reference S2V samples are constructed by pairing multiple subject references with the same target video.

G Additional Qualitative Results

We present additional qualitative results showcasing TIDE’s capabilities across diverse editing types and subject-to-video generation scenarios.

G.1 Multi-Reference Video Editing Cases

Figures 10 to 13 illustrate TIDE’s multi-reference video editing results across different editing operation combinations, including single-reference addition, background change with removal, dual object removal, and object removal with replacement.

G.2 Subject-to-Video Generation Cases

Figure 14 shows additional subject-to-video generation results on OpenS2V, demonstrating TIDE’s ability to faithfully preserve the visual identity of both human and object reference subjects while following text prompts.

Instruction: Add the beige, rectangular, textured floor rug from Image-1 underneath the black wooden chair in Video-1. The rug should be positioned flat on the dark wood floor, centered beneath the chair's legs, covering the area directly under the seating space.



Figure 10: Single-reference object addition on TIDE-Bench.

Instruction: Replace the entire library bookshelf background in Video-1 with the futuristic cityscape from Image-1, featuring tall, interconnected glass towers and elevated highways at sunset. Remove the dark blue upholstered armchair located at the center of the video where the man is sitting, leaving the man to appear as if he is floating or sitting on an invisible support in front of the new futuristic background.

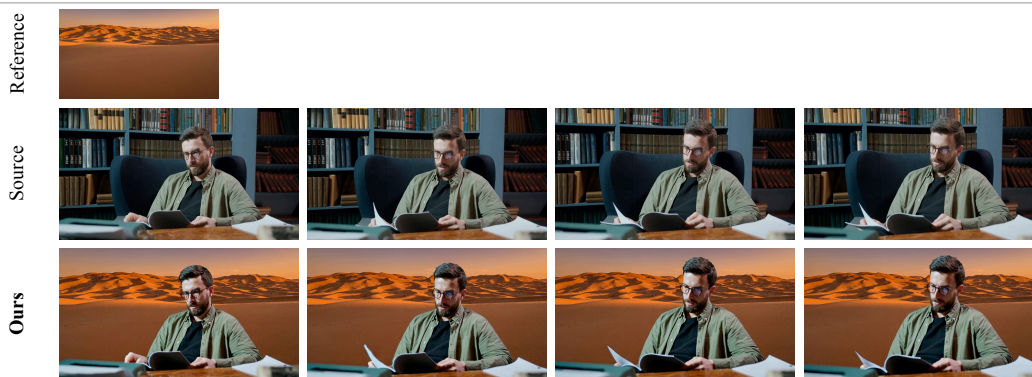


Figure 11: Multi-reference editing: background change + object removal.

Instruction: Remove the weathered brown wooden signpost located on the right side of the hiking trail in Video-1, as shown in Image-1. Additionally, remove the blue water bottle tucked into the side pocket of the blue backpack worn by the hiker in the center of Video-1, as shown in Image-2.



Figure 12: Multi-reference editing: dual object removal.

Instruction: Remove the small green potted plant located on the kitchen counter in the background of Video-1, as shown in Image-1. Replace the dark gray sofa on which the man is sitting with the brown leather armchair from Image-2, maintaining the same position and orientation in the room.

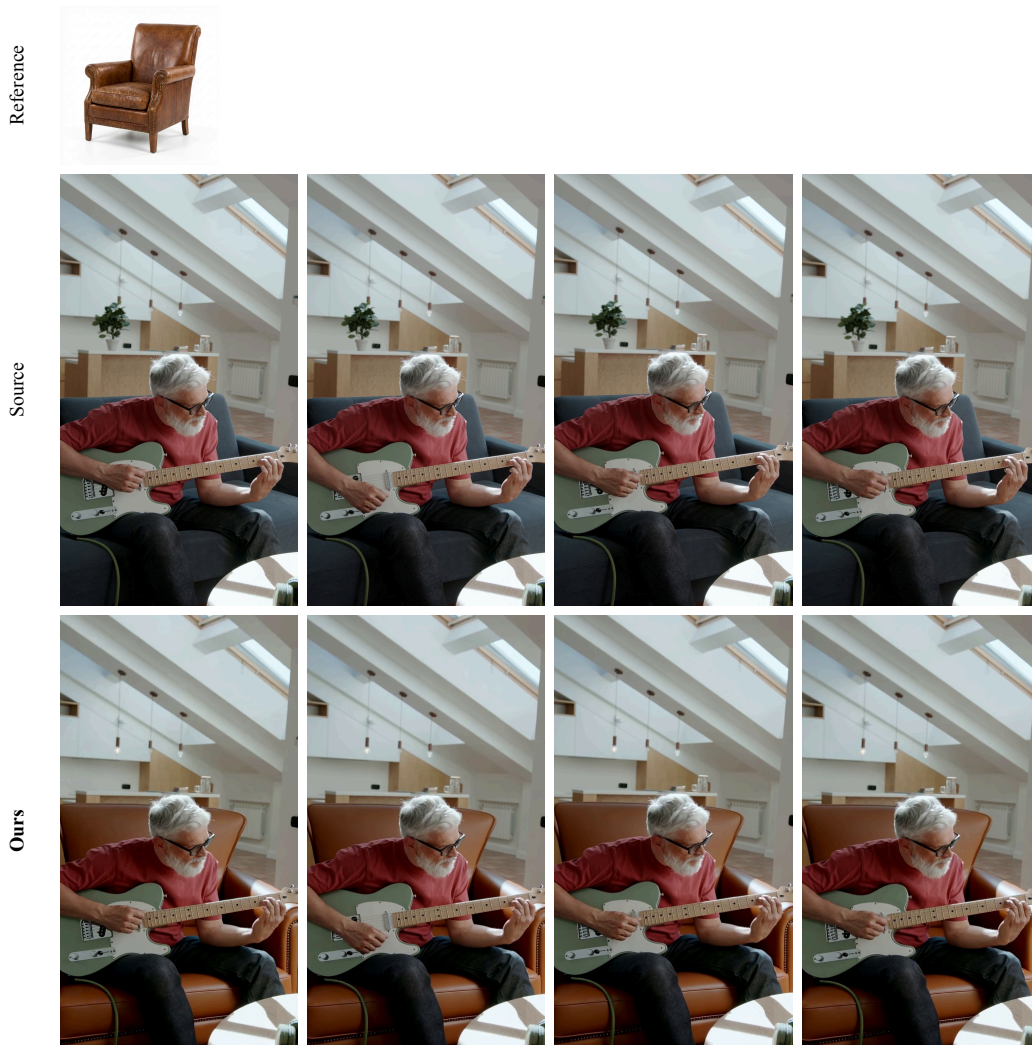


Figure 13: Multi-reference editing: object removal + replacement.

Instruction: a man feeding a bird in the park.



Instruction: The video begins with a close-up of a vintage camera resting on an old wooden desk, surrounded by scattered photographs. The camera zooms in to capture the details of the camera—its weathered leather, brass accents, and the glass lens catching the light. A hand gently picks up one of the photographs, flipping it over to reveal its back. The camera shifts focus between the photos and the camera, as the hand adjusts the camera's settings with a soft click. As the hand places the photo back onto the desk, a slight breeze causes a few of the scattered photographs to shift, creating subtle motion in the scene. The soft sound of the camera's dials and the faint rustle of paper add to the nostalgic atmosphere of the moment.



Instruction: The video depicts an indoor scene where two individuals are engaged in a conversation. The setting appears to be a well-lit room with natural light streaming through large windows. The room is furnished with a wheelchair positioned near the back, suggesting it might be a medical or care facility. A desk with a laptop and some other items is visible on the right side of the frame. The person on the left, dressed in a gray uniform, is holding a tablet and gesturing with her hands while speaking. Her posture indicates she is explaining something, possibly related to the tablet's content. The individual on the right, wearing a light-colored robe, is seated and listening attentively, smiling slightly, which suggests a positive interaction. The camera remains static throughout the sequence, focusing on capturing the interaction between the two individuals. There is no noticeable camera movement such as panning or zooming. The overall atmosphere seems calm and professional, with the focus on the exchange between the two people.

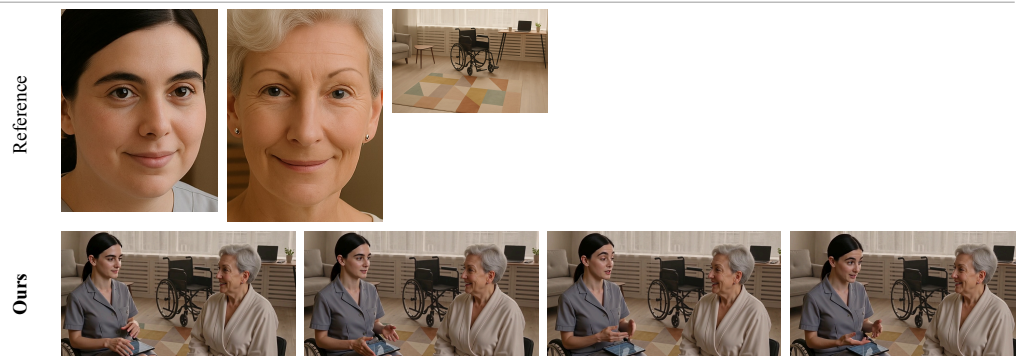


Figure 14: Subject-to-video generation on OpenS2V with human and object references.